Eigenmode changes in a misaligned triangular optical cavity

Eigenmode changes in a misaligned triangular optical cavity

F Kawazoe[1], R Schilling[2] and H Lück[1]

[1] Max-Planck-Institut für Gravitationsphysik (Albert-Einstein-Institut) und Leibniz Universität Hannover, Callinstraße 38, D-30167 Hannover, Germany
[2] Max-Planck-Institut für Gravitationsphysik (Albert-Einstein-Institut), Fröttmaninger Weg 18, D-85748 Garching, Germany

E-mail: fumiko.kawazoe@aei.mpg.de

Abstract
We derive relationships between various types of small misalignments in a triangular optical cavity and associated geometrical eigenmode changes. We focus on the changes of beam spot positions on cavity mirrors, the beam waist position and its angle. A comparison of analytical and numerical results shows excellent agreement. The results are applicable to any triangular cavity close to an isosceles triangle, with the lengths of two sides much bigger than the third, consisting of a curved mirror and two flat mirrors (the curved mirror is the distant one) yielding a waist equally separated from the two flat mirrors. This cavity shape is most commonly used in laser interferometry. The analysis presented here can easily be extended to more generic cavity shapes. The geometrical analysis not only serves as a method of checking a simulation result, but also gives an intuitive and handy tool to visualize the eigenmode of a misaligned triangular cavity.

Keywords: interferometer, alignment, ring cavity, gravitational wave

(Some figures in this article are in colour only in the electronic version)

1. Introduction

Optical cavities are widely used in the field of laser interferometry, and longitudinal length shifts of a cavity mirror and the resulting change in the phase of the resonating field are well known. However, in the case where suspended mirrors are used, such as in gravitational wave detectors, angular shifts play a crucial role in the detector performance; their knowledge ensures clean length control signals. Angular shifts of the cavity mirrors and resulting eigenmode changes in the circulating Gaussian beam of a plane cavity were geometrically analyzed in [1], and the results are used, together with results from simulation work, to obtain error signals to control the alignment of various cavity mirrors. Recently we designed a triangular optical cavity for the purpose of frequency stabilization for the AEI 10 m Prototype [2], and in the process of designing an alignment control system, a geometrical analysis for this cavity was performed. The cavity is close to an isosceles triangle, with the lengths of two sides much bigger than the third, consisting of a curved mirror

placed at the corner where the two equal sides cross, and two flat mirrors, yielding a waist halfway between the two flat mirrors. This cavity shape is most commonly used in laser interferometry, and the results presented here can easily be extended to more generic cavity shapes. In this paper we first derive the relations of small mirror misalignments and the resulting changes in the eigenmode. By small misalignments we mean the regime where a lateral shift is smaller than the waist radius and the angular deviation smaller than the divergence angle of the beam. The results are shown in terms of beam spot position changes on all the cavity mirrors, the waist position changes and the waist angular shifts. They carry sufficient information for designing an angular control system. We then compare the results with those of two simulation tools and show that they are in excellent agreement with each other.

2. Types of misalignments

Figure 1 shows the schematic of a triangular cavity when aligned. Two flat mirrors are relatively close together and are
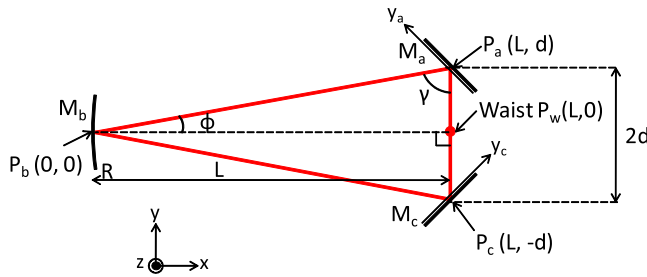
Figure 1. Schematic of an aligned triangular cavity within the $x-y$ plane. Also defined are the two coordinate axes y_a and y_c that are fixed on the flat mirrors M_a and M_c, respectively. Mirror M_b has a radius of curvature of R.
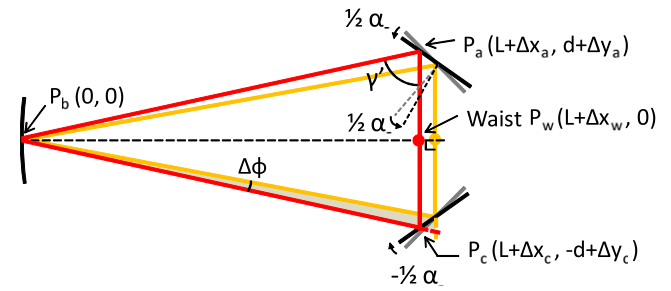
Figure 2. Cavity eigenmodes of the aligned case (lighter colored triangle) and the case misaligned by α_- (darker colored triangle). The opposite rotations around the z axis cause a symmetric change in the eigenmode.

labeled M_a and M_c, while the curved mirror is far away, has a radius of curvature R and is labeled M_b. The position where the beam hits the mirror M_i (with i standing for a, b, or c) is given by P_i, as well as the waist position by P_w, followed by the associated coordinates within the $x-y$ plane. Here, we also introduce a coordinate system attached to each of the flat mirrors (y_a and y_c) for convenience. The two equal angles of the beam at M_a and M_c and the small half-angle at M_b are given by γ and ϕ, respectively. Due to the shape of the triangle the following approximations hold and are used throughout this paper unless otherwise noted:

$$\gamma = \pi/2 - \phi \approx \pi/2 \tag{1}$$

$$\phi \ll 1. \tag{2}$$

Angular degrees of freedom in horizontal and vertical directions for the three mirrors produce six modes of misalignments.

Misalignment angles of mirror M_i are given by α_i for horizontal directions (angles around the z axis, sometimes also called yaw or rotation) and β_i for vertical directions (inclination angle with respect to the $x-y$ plane, sometimes also called pitch or tilt). A positive angle is formed by counter-clockwise rotation around the z axis for horizontal misalignments, and around the y axis, y_a axis and y_c axis for vertical misalignment of M_b, M_a and M_c, respectively. We take linear combinations of these two flat mirror misalignments to form common and differential modes: $\alpha_\pm = (\alpha_a \pm \alpha_c)$ and $\beta_\pm = (\beta_a \pm \beta_c)$ and consider equal-amount tilts for the two mirrors. The changes in the waist position and the beam spot position on mirror M_i are denoted by Δk_w and Δk_i, with k being the corresponding x or y coordinates. An angular change of the beam between the two flat mirrors is denoted by θ. Since we consider only small misalignments, these changes are also small. Hence we use the following approximation throughout this paper: $\theta \ll 1$ and $O(\Delta k^n) = 0$ for $n \geqslant 2$. All types of misalignments are summarized and the associated section numbers are listed in table 1.

3. Horizontal misalignments

3.1. Misalignment in α_-

Misalignments in α_-, i.e. opposite rotations around the z axis, keep the cavity symmetric to the x axis and, hence, cause a

Table 1. Summary of types of misalignments and associated section numbers.

Type	Description	Section
α_-	Difference of the flat mirrors in horizontal	3.1
α_b	Curved mirror in horizontal	3.2
α_+	Common of the flat mirrors in horizontal	3.3
β_b	Curved mirror in vertical	4.1
β_+	Common of the flat mirrors in vertical	4.2
β_-	Difference of the flat mirrors in vertical	4.3

symmetric change in the eigenmode. In figure 2, the original and the new eigenmodes are shown by the lighter (yellow) and darker colors (this color rule is applied throughout this paper), and the x and y coordinates of the spot positions on the mirrors are shown. Because of the symmetry it is obvious that Δx_a equals Δx_c and Δx_w, and due to the approximation given by equation (1), $|\Delta y_a|$ also equals $|\Delta x_a|$. The angle of incidence on the flat mirrors changes by $-\frac{1}{2}\alpha_-$, as indicated by the dashed normal on one mirror surface. The large angle γ' changes by $-\alpha_-$, yielding a change by α_- in half the small angle ϕ ($\Delta\phi = -\alpha_-$). From looking at the shaded area in figure 2 we get

$$\Delta y_c \approx \sqrt{L^2 + d^2} \sin\Delta\phi \approx \sqrt{L^2 + d^2} \cdot \Delta\phi$$
$$= -\sqrt{L^2 + d^2} \cdot \alpha_-. \tag{3}$$

Therefore we derive the following relations between the spot position changes and the misalignment angle:

$$\Delta x_a = \Delta x_c = -\Delta y_a = \Delta y_c = \Delta x_w = -\sqrt{L^2 + d^2} \cdot \alpha_- \tag{4}$$

and hence the angle deviation θ at the waist is zero.
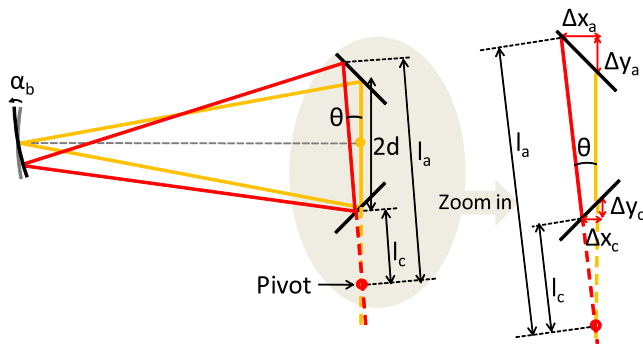
To summarize, a misalignment in $+(-)\alpha_-$ causes a shrink (stretch) of the eigenmode along the x axis, yielding the eigenmode to keep its isosceles shape, but change its shape in a way that it becomes more 'fat' ('thin'). As a result, the waist position shifts in the x direction by an amount that is approximately proportional to the distance between the curved mirror and the two flat mirrors.

3.2. Misalignment in α_b

Figure 3 shows a hypothetical misaligned cavity caused by α_b, i.e. a rotation of M_b around the vertical axis. In this case, there
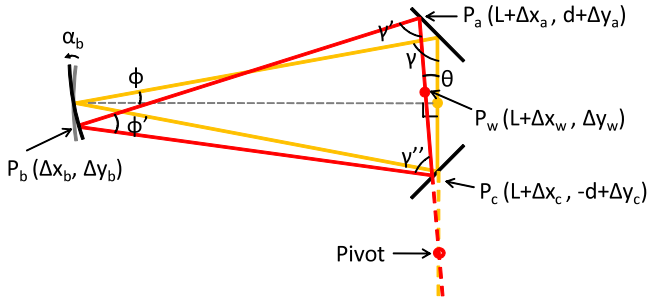
Figure 3. Cavity eigenmodes of the aligned and the misaligned cases by α_b. We start with a general, and hence hypothetical, case where the pivot and the bisecting point of the non-congruent side do not match, and later show that they do coincide. The changes of the two larger angles (γ) are of equal size but with opposite sign, hence the small angle ϕ' stays unchanged.

Figure 4. Closer view of the two flat mirrors and the pivot. It still shows the hypothetical eigenmode where the pivot and the bisecting point do not match.

Figure 5. Closer view of the two flat mirrors. Here, the pivot and the bisecting point coincide, and the y coordinate of the pivot is denoted by Δy_p.
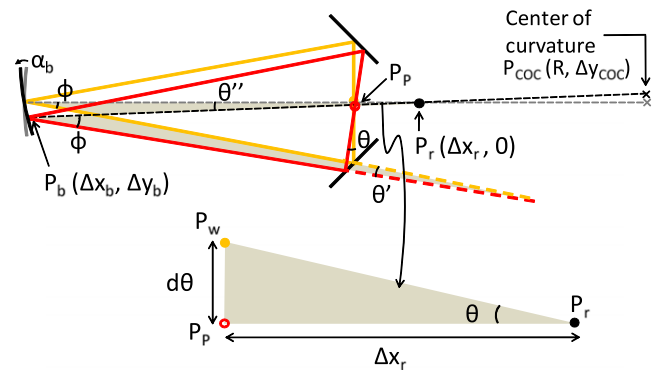
Figure 6. Radius vectors of the aligned and the misaligned cases. They cross at the point P_r, from which the angle deviation and the pivot location are calculated.

is no obvious symmetry axis. One can expect changes in the positions of the beam spots on the mirrors and of the waist, as well as an angle deviation at the waist. We introduce a pivot, where the non-congruent side of the aligned and the misaligned eigenmodes cross, indicated by the thick circle. We start with an arbitrary location of the pivot, and will shortly show that it coincides with the bisecting point of the non-congruent side.

The angle of incidence on the flat mirrors changes by the same amount θ, but with opposite sign, resulting in the following changes of the large angles: $\gamma' = \gamma + 2\theta$ and $\gamma'' = \gamma - 2\theta$. Hence the small angle stays unchanged: $\phi' = 2\phi$.

Looking at the flat mirrors, as shown in figure 4, and applying the approximation given by equation (1), one sees that $\Delta x_a = -\Delta y_a$ and $\Delta x_c = \Delta y_c$. The following set of equations describes the shift of the spot positions:
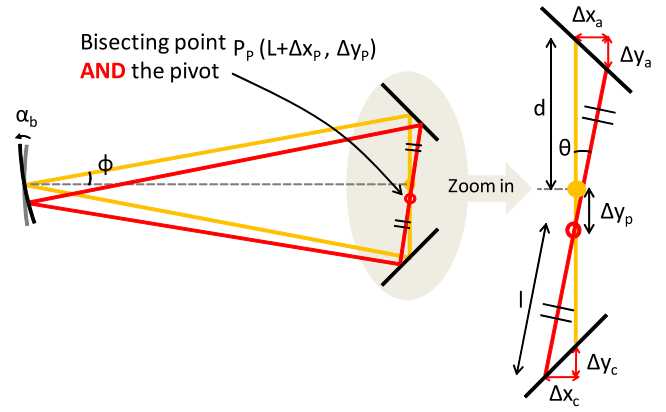
$$\Delta x_a = l_a \sin \theta \tag{5}$$

$$\Delta x_c = l_c \sin \theta \tag{6}$$

$$2d = l_a \cos \theta - l_c \cos \theta - |\Delta y_a| - |\Delta y_c| \tag{7}$$

$$= (l_a - l_c) \cos \theta - (|\Delta x_a| + |\Delta x_c|)$$

$$\approx l_a - l_c - (|l_a| + |l_c|)\theta \tag{8}$$

where l_a and l_c are the distances from the pivot to P_a and P_c along the beam, respectively. The left-hand side of equation (7)

is constant, hence the right-hand side must be independent of θ, yielding the following relations:

$$l_a = -l_c \tag{9}$$

$$|l_a| = |l_c| = d/\cos \theta \equiv l \tag{10}$$

$$\Delta x_a = -\Delta x_c = -\Delta y_a = -\Delta y_c = -l \sin \theta$$

$$= -d \tan \theta \approx -d\theta. \tag{11}$$

This automatically means that the pivot (P_p) bisects the non-congruent side, as shown in figure 5, where the changes in the location of the pivot are denoted by Δx_p and Δy_p. It also shows the details around the flat mirrors, from which the pivot location with respect to the original waist is given by

$$\Delta x_p = O(\theta^2) = 0 \tag{12}$$

$$\Delta y_p = d - l \cos \theta + \Delta y_a = d\theta \tag{13}$$

Connecting the beam spot on the curved mirror (P_b) and the bisecting point (the pivot, or P_p), one can see that it bisects the beam angle at M_b into ϕ, as shown in figure 6. This means that the line passes through the center of curvature, (P_{coc}), whose coordinate along the y axis is given by

$$\Delta y_{coc} = R \cdot \alpha_b. \tag{14}$$
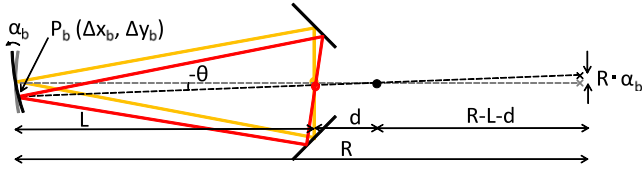
Figure 7. Length information needed to calculate θ and the spot position change on M_b.
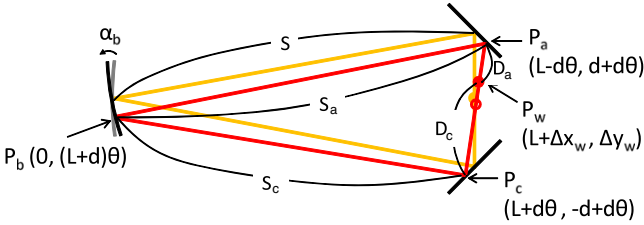
Figure 8. Locations of the new spot positions on the mirrors. By using them the new waist location is calculated.

Focusing on the shaded triangles shown in figure 6, one can see that $\theta' = -\theta$ and, comparing the two triangles, one can also see that $\theta'' = \theta' = -\theta$. The radius vectors of the aligned and misaligned mirrors, indicated by the dotted lines in figure 6, cross at point P_r. By focusing on the triangle consisting of the original waist (P_w), the pivot (P_p) and P_r, as shown in the lower triangle in figure 6, one can see that the x coordinate of the point P_r is given by

$$\Delta x_r = d\theta / \tan\theta \approx d. \tag{15}$$

Figure 7 lists all the length information that is needed to calculate the angle θ and the spot position on M_b. These are given by the following set of equations:

$$\theta \approx \tan\theta = -R\alpha_b/(R - L - d) \tag{16}$$

$$\Delta x_a \approx dR\alpha_b/(R - L - d) \tag{17}$$

$$\Delta x_b = \mathrm{O}(\Delta y_b^2) = 0 \tag{18}$$

$$\Delta y_b = -(L + d)\tan{-\theta} \approx (L + d)\theta$$
$$= R\alpha_b \cdot (L + d)/(R - L - d). \tag{19}$$

Having calculated the new spot positions on the mirrors, we now calculate where the new waist is. In order for the wavefront curvature of the beam to match the radius of curvature of the curved mirror M_b, the path lengths from the waist to the mirror M_b via M_a and via M_c should be the same, i.e. in figure 8 it should be $S_a + D_a = S_c + D_c = S + d$. By calculating the distances S_a and S_c in the following equations, we also obtain the distances D_a and D_c:

$$S_a = \{(L - d\theta)^2 + (d - L\theta)^2\}^{1/2}$$
$$\approx \sqrt{L^2 + d^2}\left(1 - \frac{4Ld\theta}{L^2 + d^2}\right)^{1/2} \qquad \theta^2 = 0$$
$$\approx \sqrt{L^2 + d^2}\left(1 - \frac{2L\,d\theta}{L^2 + d^2}\right) \qquad \frac{2Ld\theta}{L^2 + d^2} \ll 1$$
$$= S - 2\,d\theta \qquad d^2/L^2 = 0 \tag{20}$$
$$D_a = S + d - S_a = d + 2\,d\theta \tag{21}$$
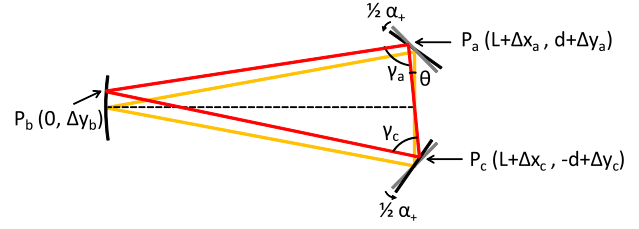
Figure 9. Cavity eigenmodes of the aligned and the misaligned (α_+) cases.
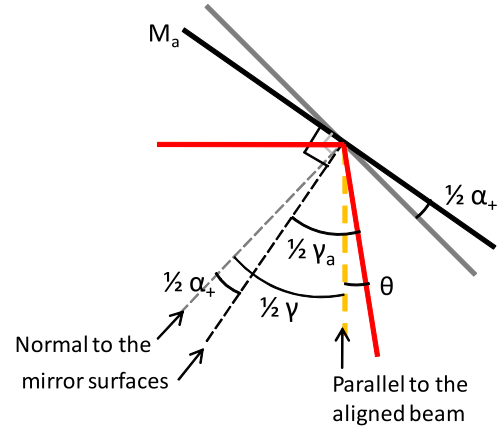
Figure 10. Closer view on the change in one of the larger angles, γ_a.

In a similar way

$$S_c = \{(L + d\theta)^2 + (-d - L\theta)^2\}^{1/2} = S + 2\,d\theta \tag{22}$$

$$D_c = S + d - S_c = d - 2\,d\theta. \tag{23}$$

Hence, the new waist location is given by the following:

$$\Delta x_w = \mathrm{O}(\theta^2) = 0 \tag{24}$$

$$\Delta y_w = (d + d\theta - D_a)\cos{-\theta} \approx -d\theta = -dR\alpha_b/(R - L - d). \tag{25}$$

To summarize, a misalignment in $+(-)\alpha_b$ causes a clockwise (counter-clockwise) rotation of the non-congruent side around the bisecting point, yielding the long sides to rotate synchronously. As a result all the beam spot positions change by the amounts given by the radial distances, with the bisecting point being the origin of the system of radial coordinates.

3.3. Misalignment in α_+

In the case of α_+, i.e. concordant rotations around the z axis, there is no obvious symmetry line, thus we will start from a general case. Changes in the spot positions, the beam angle at the waist and the two larger angles are defined as shown in figure 9. Figure 10 focuses on the beam angle change on mirror M_a. Drawing helping lines, such as the one that is parallel to the aligned beam (indicated by the light colored thick dotted line), as well as lines that are normal to both the aligned and the misaligned mirror surfaces (indicated by the
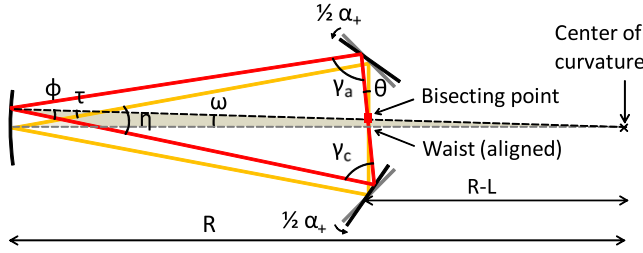
Figure 11. Ancillary angles: β, η and ω, which are used to calculate θ.

Figure 12. Yet another ancillary angle γ_a' to calculate η.

light thin and dark thin dotted lines, respectively), one can see that half of γ_a is given by $\gamma_a/2 = \gamma/2 + \theta - \alpha_+/2$. Hence

$$\gamma_a = \gamma + (2\theta - \alpha_+). \tag{26}$$

In a similar manner, γ_c is given by

$$\gamma_c = \gamma - (2\theta - \alpha_+). \tag{27}$$

This means that the sum of the two angles stays unchanged, yielding no change in the small angle ϕ'. Then the line that connects P_b with the center of curvature of M_b (from here on this is called the *radius*) should bisect the short side, due to the fact that $d \ll L$. The bisecting point is indicated by the square point in figure 11. Here, we introduce some ancillary angles τ and η, together with ω, which is the angle of the radius with respect to the aligned case. Focusing on the shaded area, one can see that the ancillary angles are given by

$$\tau = \phi + \omega \qquad \text{and} \tag{28}$$

$$\eta = \phi + \tau = 2\phi + \omega. \tag{29}$$

η can be expressed using γ if one focuses on the shaded triangle shown in figure 12, introducing a new ancillary angle $\gamma_a' = \gamma + \theta$, and it is given by

$$\eta = \pi - (\gamma_a' + \gamma_c) = \pi - \{(\gamma + \theta) + \gamma - (2\theta - \alpha_+)\}$$
$$= \pi - 2\gamma + \theta - \alpha_+. \tag{30}$$

By comparing equations (29) and (30) the angle ω is given by the following equations:
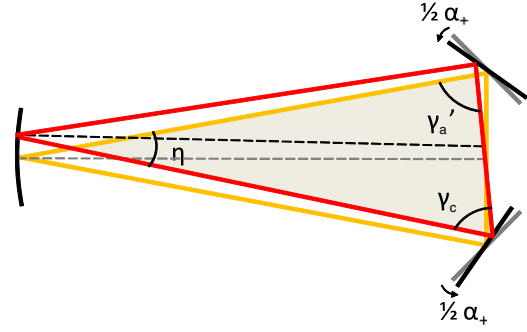
$$\pi - 2\gamma + \theta - \alpha_+ = 2\phi + \omega \tag{31}$$

$$\omega = \pi - (2\gamma + 2\phi) + \theta - \alpha_+ = \theta - \alpha_+. \tag{32}$$
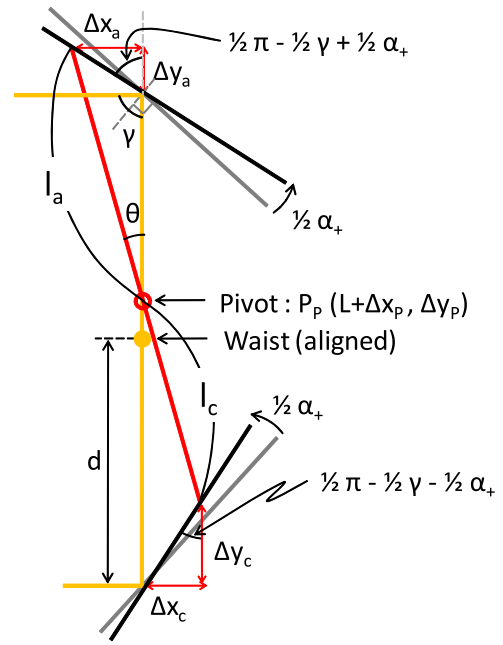
In order to gain additional information to finally calculate θ, we focus on some lengths as shown in figure 13. The pivot (P_p) is indicated by the thick circle and changes in its location are denoted by Δx_p and Δy_p, and the two lengths from the pivot to the two beam spots by l_a and l_c. Changes in coordinates of the beam spot position on M_a are given by the following equations:

$$\Delta x_a = -l_a \sin\theta \approx -l_a\theta \tag{33}$$

$$\Delta y_a = \frac{-\Delta x_a}{\tan(\pi/2 - \gamma/2 + \alpha_+/2)} \approx \frac{1 - \alpha_+/2}{1 + \alpha_+/2}l_a\theta$$
$$\approx (1 - \alpha_+)l_a\theta \tag{34}$$

Figure 13. Length relations around the flat mirrors. From this the lengths l_a and l_c from the pivot to the beam spots on the two mirrors are calculated.

and Δx_c and Δy_c by

$$\Delta x_c = l_c \sin\theta \approx l_c\theta. \tag{35}$$

$$\Delta y_c = \frac{\Delta x_c}{\tan(\pi/2 - \gamma/2 - \alpha_+/2)} \approx \frac{1 + \alpha_+/2}{1 - \alpha_+/2}l_c\theta$$
$$\approx (1 + \alpha_+)l_c\theta. \tag{36}$$

The length of the non-congruent side is then expressed by the following:

$$2d = l_a \cos\theta + \Delta y_a + l_c \cos\theta + \Delta y_c$$
$$\approx l_a + l_c - \{l_a - l_c - (l_a + l_c)\alpha_+\}\theta. \tag{37}$$
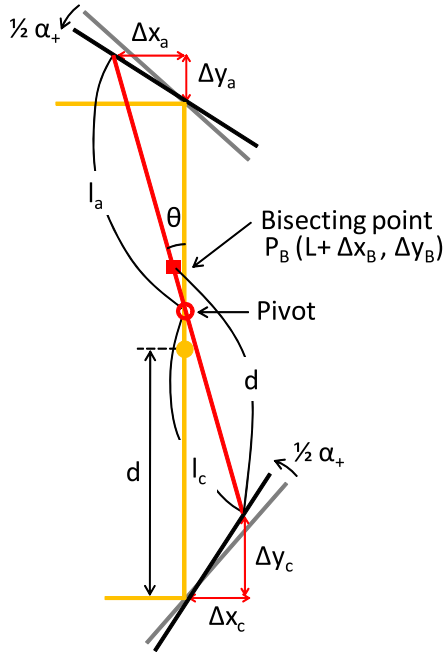
Since the left-hand side of equation (37) does not depend on the misalignment angle θ, the angle-dependent term of the right-hand side should be zero, hence

$$l_a - l_c - (l_a + l_c)\alpha_+ = 0. \tag{38}$$

From equations (37) and (38) the following relations can be obtained:

$$l_a = d(1 + \alpha_+) \tag{39}$$

$$l_c = d(1 - \alpha_+). \tag{40}$$

Figure 14. Length relations around the flat mirrors, including the pivot location. From this the spot position changes on the flat mirrors are calculated.

With this knowledge we can calculate the location of the pivot in the following way:

$$\Delta x_p = O(\theta^2) = 0 \tag{41}$$

$$\Delta y_p = l_c \cos\theta + \Delta y_c - d \approx d(\theta - \alpha_+). \tag{42}$$

The location of the bisecting point, as shown in figure 14, can be calculated in a similar way and the coordinates are given by

$$\Delta x_B = O(\theta^2) = 0 \tag{43}$$

$$\Delta y_B = d\cos\theta + \Delta y_c - d \approx (1 + \alpha_+)(1 - \alpha_+)\, d\theta \approx d\theta. \tag{44}$$

Then, focusing on the triangle that consists of the center of curvature, the waist (in the aligned case), and the bisecting point (indicated by the right part of the shaded area in figure 11), one can obtain another relation for ω and θ which is given by
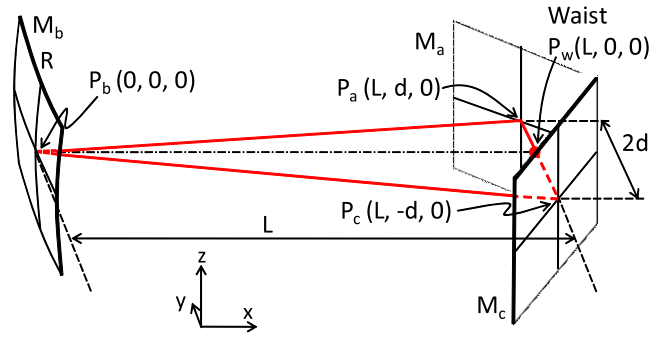
$$\omega \approx \tan\omega = d\theta/(R - L). \tag{45}$$

From equations (32) and (45) one can finally obtain the relation between θ and α_+:

$$\theta = \frac{R - L}{R - L - d} \cdot \alpha_+. \tag{46}$$

Using θ, the spot positions on the three mirrors (see equations (33)–(36)) can further be calculated. This yields the following equations:

$$\Delta x_a = -d(1 + \alpha_+)\theta \approx -\frac{d(R - L)}{R - L - d} \cdot \alpha_+ \tag{47}$$

$$\Delta y_a = (1 - \alpha_+)\Delta x_a \approx \frac{d(R - L)}{R - L - d} \cdot \alpha_+. \tag{48}$$

Figure 15. 3D view of a triangular cavity. M_a and M_c are the flat mirrors, and M_b has a radius of curvature of R. The position where the beam hits the mirror M_i is denoted by P_i.

And in similar ways

$$\Delta x_c = \frac{d(R - L)}{R - L - d} \cdot \alpha_+ \tag{49}$$

$$\Delta y_c = \frac{d(R - L)}{R - L - d} \cdot \alpha_+ \tag{50}$$

and

$$\Delta x_b = O(\Delta y_b^2) = 0 \tag{51}$$

$$\Delta y_b = R \cdot \omega = R \cdot (\theta - \alpha_+) = \frac{dR}{R - L - d} \cdot \alpha_+. \tag{52}$$

Then the waist location can be calculated in the same way as shown in equations (20)–(25), and the following can be shown:

$$S_a = \{(L + \Delta x_a)^2 + (d + \Delta y_a - \Delta y_b)^2\}^{1/2} \approx S - (d\theta + \Delta y_p) \tag{53}$$

$$D_a = d + d\theta + \Delta y_p. \tag{54}$$

In a similar way we obtain

$$S_c = S + (d\theta + \Delta y_p) \tag{55}$$

$$D_c = d - d\theta - \Delta y_p. \tag{56}$$

Therefore the new waist location is given by

$$\Delta x_w = O(\theta^2) = 0 \tag{57}$$

$$\Delta y_w = (d + \Delta y_a - D_a)\cos\theta \approx -\Delta y_p = -\frac{d^2}{R - L - d} \cdot \alpha_+. \tag{58}$$

To summarize, a misalignment in $+(-)\alpha_+$ causes a counter-clockwise (clockwise) rotation of the non-congruent side around a point that does not coincide with the bisecting point. This yields a clockwise (counter-clockwise) rotation ω (which is very small compared to the misalignment angle α_+) of the geometrical axis of a corner reflector consisting of the two flat mirrors. As a result, the eigenmode changes in a 'non-uniform' way, with each spot position change being smaller than the misalignment case of α_b.

4. Vertical misalignments

When considering vertical misalignments, it is necessary to view the cavity as a 3D body, as shown in figure 15. Notations of all the properties are the same as those shown in figure 1.
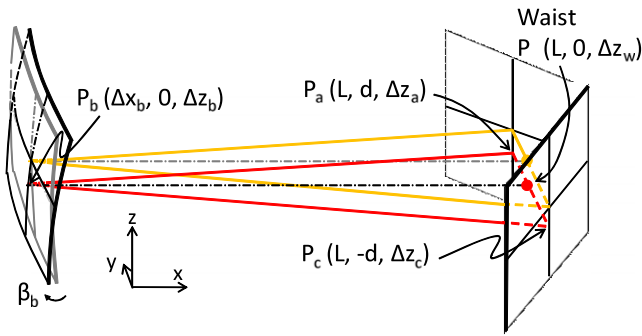
Figure 16. Cavity eigenmodes of the aligned (lighter colored triangle) and the misaligned by β_b (darker colored triangle) cases. This type of misalignment does not affect the mirror alignment in the y direction, hence the eigenmode changes only along the z axis.
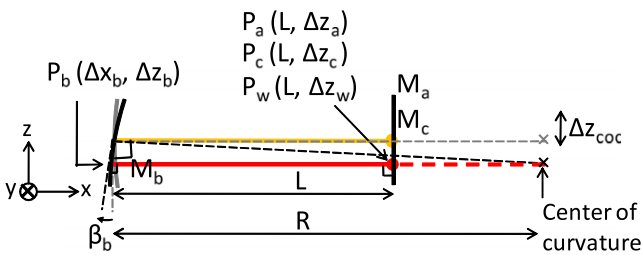
Figure 17. Projection of the triangular cavity onto the x–z plane. It allows one to view the cavity as a plane cavity. The eigenmode is defined by the line that is orthogonal to the flat mirror and passes through the center of curvature.

4.1. Misalignment in β_b

A misalignment around the y axis by β_b, as shown in figure 16, does not affect the mirror alignment in the y direction, hence there is no change in eigenmode in that direction. Then it is possible to project the cavity onto the x–z plane for simplicity, as shown in figure 17, and treat it as a plane cavity. The eigenmode of the cavity is defined by the line that is orthogonal to the flat mirrors and passes through the center of curvature, as described in [1]. It is obvious that the eigenmode is also orthogonal to the curved mirror, yielding the shifts in z direction of all of the spot positions to have the same size. The normal vector on the mirror M_b is tilted by β_b, hence the center of curvature, whose z coordinate is denoted by z_{coc}, shifts by $\Delta z_{coc} = -\beta_b \cdot R$. Therefore we have the following relations:

$$\Delta x_a = O(\beta_b^2) = 0 \tag{59}$$

$$\Delta z_a = \Delta z_b = \Delta z_c = \Delta z_w = \Delta z_{coc} = -\beta_b \cdot R. \tag{60}$$

To summarize, a misalignment in $+(-)\beta_b$ causes an downward (upward) shift of the center of curvature along the z axis, yielding a simultaneous shift of the plane of the eigenmode by an amount proportional to the radius of curvature of the curved mirror.

4.2. Misalignment in β_+

Similar to β_b, β_+ has no effects in the y direction, as shown in figure 18. However, since the y_a axis and the y_c axis are
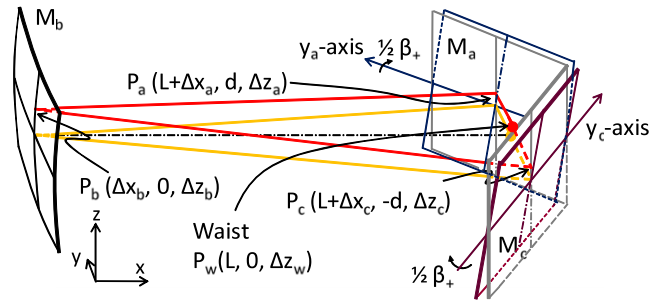
Figure 18. Cavity eigenmodes of the aligned and the misaligned (β_+) cases. This type of misalignment does not affect the mirror alignment in the y direction, hence the eigenmode changes only along the z axis.
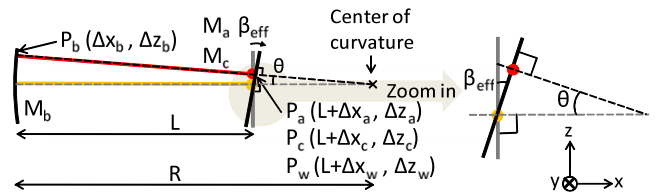
Figure 19. Projection of the triangular cavity onto the x–z plane. It allows one to view the cavity as a plane cavity. The eigenmode is defined by the line that is orthogonal to the flat mirrors and passes through the center of curvature. In the right part, an enlarged cut-out around one flat mirror is shown.

rotated by $\pm(\frac{\pi}{2} - \frac{\gamma}{2}) \approx \pm\frac{\pi}{4}$ around the z axis with respect to the y axis, respectively, the projection of a misalignment by $\beta_+/2$ around the two axes becomes $\frac{1}{2}\beta_+/\sqrt{2}$. Section 4.10 (pp 100–102) of [3] gives a detailed explanation of this effect by using vector algebra and we will not describe it in this paper. For convenience, we introduce an effective misalignment angle $\beta_{eff} = \beta_+/\sqrt{2}$. The projection of the flat mirrors is rotated by $\beta_{eff}/2$ around the y axis and the effect is doubled because of the two reflections; hence, seen as a plane cavity, the misalignment angle is given by β_{eff}, as shown in figure 19. The eigenmode of this cavity is defined by the line that passes through the center of curvature and intersects the flat mirrors orthogonally, as described in [1]. The angle formed by the eigenmodes of the aligned and misaligned cases is denoted by θ in figure 19 and it becomes obvious that $\theta = \beta_{eff}$ when one focuses around the area of the flat mirrors, as shown in the enlarged cut-out in the right part of figure 19. Therefore the following equations yield the spot position changes:

$$\Delta x_{a,b,c, \text{ and w}} = O(\beta_+^2) = 0 \tag{61}$$

$$\Delta z_a = \Delta z_c = \Delta z_w = \beta_{eff} \cdot (R - L) = \beta_+ \cdot (R - L)/\sqrt{2} \tag{62}$$

$$\Delta z_b = \beta_{eff} \cdot R = \beta_+ \cdot R/\sqrt{2}. \tag{63}$$

To summarize, a misalignment in $+(-)\beta_+$ causes a counter-clockwise (clockwise) tilt of the geometrical axis of the two flat mirrors around the center of curvature. As a result the cavity plane tilts around the y axis through the center of curvature.

Table 2. Horizontal misalignment comparison.

Type	Method	M_a Δx	Δy	M_c Δx	Δy	M_b Δx	Δy	Waist Δx	Δy	θ
α_b	Geom. analy.	0.205	−0.205	−0.205	−0.205	0	−13.970	0	0.205	−1.370
	OPTOCAD	0.206	−0.202	−0.206	−0.202	0	−13.974	0	0.209	−1.370
	IFOCAD	0.206	−0.202	−0.206	−0.202	0	−13.974	0	0.209	−1.370
α_-	Geom. analy.	−10.051	10.051	−10.051	−10.051	0	0	−10.051	0	0
	OPTOCAD	−10.051	9.902	−10.051	−9.902	0	0	−10.051	0	0
	IFOCAD	−10.051	9.902	−10.051	−9.902	0	0	−10.051	0	0
α_+	Geom. analy.	−0.151	0.151	0.151	0.151	0	0.205	0	−0.001	1.005
	OPTOCAD	−0.151	0.149	0.151	0.149	0	0.206	0	−0.003	1.005
	IFOCAD	−0.151	0.149	0.151	0.149	0	0.206	0	−0.003	1.005

Table 3. Vertical misalignment comparison.

Type	Method	M_a Δx	Δz	M_c Δx	Δz	M_b Δx	Δz	Waist Δx	Δz	θ
β_b	Geom. analy.	0	−37.800	0	−37.800	0	−37.800	0	−37.800	0
	IFOCAD	0	−37.800	0	−37.800	0	−37.800	0	−37.800	0
β_-	Geom. analy.	0	−0.106	0	0.106	0	0	0	0	0.707
	IFOCAD	0	−0.106	0	0.106	0	0	0	0	0.702
β_+	Geom. analy.	0	19.622	0	19.622	0	26.729	0	19.622	0
	IFOCAD	0	19.770	0	19.770	0	26.930	0	19.770	0
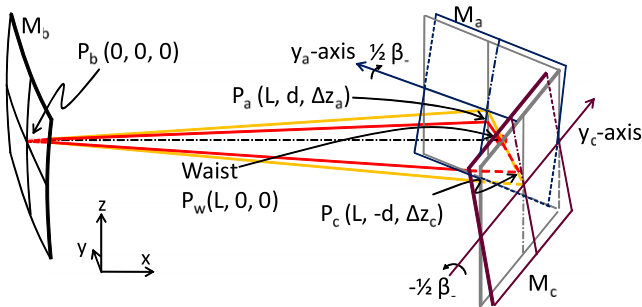
Figure 20. Cavity eigenmodes of the aligned and the misaligned (β_-) cases. The beam spot position and the waist position stay unchanged.

Figure 21. Projection of the triangular cavity onto the y–z plane. The plane of the cavity is rotated around the x axis by θ. However, the lengths of all sides of the triangle remain unchanged.

4.3. Misalignment in β_-

Here, mirrors M_a and M_c rotate around the y_a and y_c axes by $\pm 1/2\beta_-$, respectively, as shown in figure 20. When the two opposite misalignment angles on mirrors M_a and M_c are projected onto the x–z plane, they appear as rotations around the y axis by $\pm\beta_{\rm eff}/2$, respectively, yielding no change along the z axis on the curved mirror M_b. On the other hand, when they are projected onto the y–z plane, as shown in figure 21, they both appear as rotations around the z axis by $\beta_{\rm eff}/2$, yielding shifts along the z axis in the beam spot positions on the two flat mirrors by the same amount, but with opposite sign. Note that here $\beta_{\rm eff} \equiv -\beta_-/\sqrt{2}$. These spot position changes are symmetrical along the y axis, thus they yield no change in the beam spot position on the curved mirror along the y axis, nor a change in the waist position (which is equidistant from the two spot positions) along the y axis and x axis. Hence the spot on the curved mirror and the waist remains unchanged, indicating that the new eigenmode is formed by rotating the aligned eigenmode around the x axis by θ, yielding no change in the lengths on any sides of the triangle.

The inclination angle of the beam between the two flat mirrors with respect to the x–y plane is denoted by θ in figure 21. Focusing on the isosceles triangle, as indicated by the shaded triangle in the figure, whose equal angles are denoted as μ, the inclination angle is given by the following equations:

$$\mu = \pi/2 + \beta_{\rm eff}/2 \tag{64}$$

$$\theta = \pi - 2\mu = -\beta_{\rm eff}. \tag{65}$$

Therefore the beam spot position shifts on the two mirrors are calculated to be

$$\Delta z_a = -\Delta z_c = d \cdot \beta_{\rm eff} = -d \cdot \beta_-/\sqrt{2}. \tag{66}$$

To summarize, a misalignment in $+(-)\beta_-$ causes no change in the spot position on the curved mirror and a clockwise (counter-clockwise) rotation of the non-congruent side around the x axis. As a result, the plane of the eigenmode rotates around the x axis.

5. Result and comparison

Tables 2 and 3 show the results from the geometrical analysis, and compare them to the simulation results obtained by using two simulation tools. The values are the proportionality coefficients and have units of m rad^{-1} for spot positions and rad rad^{-1} for angles. One is OPTOCAD [4] and the other is IFOCAD [5]. We used them to trace the Gaussian beam through our triangular cavity model that has the design parameters for the AEI 10 m Prototype reference cavity. These parameters are given as follows: $R = 37.8$ m, $L = 10.05$ m and $d = 0.15$ m. By inserting these values into our geometrical model, we obtained the corresponding numerical values. Due to the fact that OPTOCAD is two-dimensional we used it for simulating only the horizontal misalignment types.

6. Conclusion

The discrepancies between the geometrical analysis and the simulations are divided into two groups: one comes from the first-order effect caused by using $\gamma = \pi/2$ instead of assigning the real value, while the other comes from the non-first-order effects. The discrepancies for the beam positions on the two flat mirrors in the horizontal direction and all of the discrepancies in the vertical direction belong to the former group. Thus they become zero by assigning the real value for γ. The beam position on the curved mirror and the waist position in the horizontal direction belong to the latter group. Thus they are not completely eliminated by assigning the real value for γ. However, all of the discrepancies shown in the tables are negligible for the design of an alignment control system for a triangular cavity, due to the fact that couplings of residual alignment noise caused by these discrepancies into length control signals are negligible. The results of the geometrical analysis are in excellent agreement with the simulation results, showing sufficient accuracy for the design of an alignment control system for a triangular cavity. This analysis can easily be extended to a cavity with a more general shape if one follows the equations derived in this paper and modifies the method of approximation properly. The geometrical analysis not only serves as a method of checking a simulation result but also gives an intuitive and handy tool to visualize the eigenmode of a misaligned triangular cavity.

Acknowledgments

References

[1] Heinzel G 1999 Advanced optical techniques for laser-interferometric gravitational-wave detectors *PhD Thesis* ftp.rzg.mpg.de/pub/grav/ghh/ghhthesis.pdf

[2] Kawazoe F *et al* 2010 Designs of the frequency reference cavity for the AEI10 m prototype interferometer *J. Phys. Conf. Ser.* **228** 012028

[3] Freise A 2010 Frequency domain INterfErometer Simulation SotfwarE *FINESSE Manual* http://www.gwoptics.org/finesse/download/Finesse-0.99.8.pdf

[4] OPTOCAD (0.90c) 2010 A Fortran95 module for tracing Gaussian TEM$_{00}$ beams through an optical set-up, written by Roland Schilling *Simulation Tool* http://www.rzg.mpg.de/~ros/optocad.html

[5] IFOCAD 2010 A framework of C subroutines to plan and optimize the geometry of laser interferometers, written by Gerhard Heinzel *Simulation Tool*